Coherent Thermal Antenna Using a Photonic Crystal Slab

M. Laroche, R. Carminati, and J.-J. Greffet

Laboratoire d'Énergétique Moléculaire et Macroscopique, Combustion, École Centrale Paris, Centre National de la Recherche Scientifique, Grande Voie des Vignes, 92295 Châtenay-Malabry Cedex, France

(Received 4 October 2005; published 30 March 2006)

We show that a photonic crystal film can emit coherent thermal radiation. We demonstrate the key role of leaky waves existing at the air-photonic crystal interface. The frequency and direction of emission depend on the lattice parameters. This paves the way towards the design of coherent infrared antennas.

DOI: 10.1103/PhysRevLett.96.123903 PACS numbers: 42.70.Qs, 42.25.Kb, 42.72.Ai, 44.40.+a

Control of thermal emission of radiation has become a key issue in a lot of applications such as thermophotovoltaics. For instance, microstructured surfaces exhibit spectrally selective thermal emission [1–3]. Surface waves have been shown to play a key role in the spatial coherence of thermal sources [4–6]. Recently, the control of thermal emission of photonic crystals has drawn much attention [7–13]. Lin *et al.* have demonstrated that they could tailor the emissivity of a 3D photonic crystal of tungsten [7,8]. Studies on 1D photonic crystal have also shown that the emission properties of multilayers could be modified [9–13]. Surface waves on photonic crystals [14–16] can be used to mimic plasmonics [17–19]. Such a metamaterial has several advantages: (i) the operating frequency can be tuned by changing the lattice periodicity; (ii) there are surface waves for both polarizations [14,16]; (iii) depending on the application, transparent or lossy materials can be used.

In this Letter, we show that a lossy photonic crystal slab can generate coherent thermal emission in the near infrared. We demonstrate that the physical origin of coherent emission is the excitation of leaky waves on the interface separating air from the photonic crystal. The surface-wave dispersion relation depends on the lattice parameters, so that the emission frequency and direction can be changed. This is a key result which should lead to the design of tunable infrared antennas.

This study investigates the emission properties of a photonic crystal of germanium (Ge) in the near infrared (around 1.55 μm). In the range of wavelength studied here, $\lambda \in [1.45\ \mu\text{m}; 1.75\ \mu\text{m}]$, Ge has a complex refractive index exhibiting both a high real part and losses [20]. The geometry of the system is given in Fig. 1. It consists of a chessboard of infinitely long square rods of Ge, periodically spaced with a shift of half a period between consecutive layers and surrounded by air. The parameters are as follows: period $a = 0.95\ \mu$m, fill factor $f = 0.5$, and height of the layers $h = 0.475\ \mu$m.

With the plane-wave expansion method [21], we calculate the band structure (Fig. 2) in p polarization of the infinite photonic crystal, taking for the dielectric constant its value at $\lambda = 1.55\ \mu$m, $\epsilon_{\text{Ge}} = 18.27$ and neglecting the losses. We find a complete band gap in the range of reduced frequency $[0.59; 0.62]$ (e.g., $\lambda \in [1.53\ \mu\text{m}; 1.60\ \mu\text{m}]$), as indicated by the hatching in Fig. 2.

We now study the radiative properties of a finite film (9 layers) of this photonic crystal. With a rigorous coupled wave analysis [22], we calculate the transmission and absorption spectrum of the film. By Kirchhoff's law [23], the latter yields the emission spectrum. We first investigate the transmission spectrum of the film neglecting the losses. Figure 3(a) displays the transmissivity versus the wavelength of the incident plane wave in p polarization and for two incident angles: $\theta = 30°$ and $\theta = 70°$. The gap appears in the interval $[1.53\ \mu\text{m}; 1.60\ \mu\text{m}]$, as the transmission factor of the finite photonic crystal film is below 10^{-4}. Then, we calculate the absorption and transmission factor [Fig. 3(b)] in the same range of wavelengths for the angle $\theta = 30°$ taking into account the losses, using the data of Ref. [20]. For wavelengths larger than $\lambda = 1.55\ \mu$m, the losses in Ge are not very large (the imaginary part of the optical index is about 5×10^{-3}) so the gap is not modified. Indeed, the transmission factor is weak (less than 10^{-4}), and so is the absorptivity (less than 0.05). $\lambda = 1.55\ \mu$m is the onset of interband absorption in Ge. Below $\lambda = 1.55\ \mu$m, the gap is modified and the weak

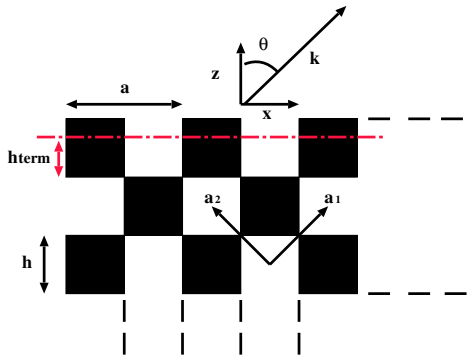

FIG. 1 (color online). Geometry of the system, period $a = 0.95\ \mu$m, $f = 0.5$, and $h = 0.475\ \mu$m. In the case of a truncated photonic crystal (indicated by the dot-dashed line), the first layer can have a different height h_{term}. θ is the emission angle. $\mathbf{a}_1$ and $\mathbf{a}_2$ are the primitive vectors of the Bravais lattice.

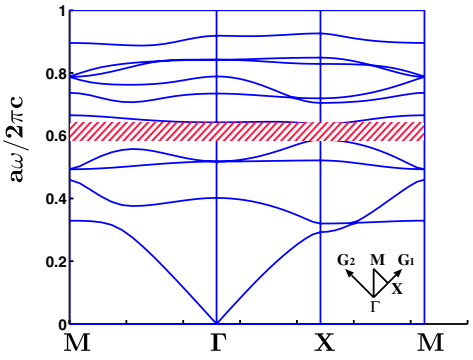

FIG. 2 (color online). Band structure of the infinite photonic crystal of Ge (approximated dielectric constant $\epsilon_{Ge} = 18.27$) in p polarization. The range of wavelengths studied in this Letter lies in the second gap around 1.55 μm corresponding to a reduced frequency of 0.613. $\mathbf{G}_1$ and $\mathbf{G}_2$ are the reciprocal lattice vectors.

transmission factor is no longer due to a high reflectivity but to a large absorption as clearly seen in Fig. 3(b).

Figure 3(c) shows the emission spectrum in the emission angle of $\theta = 33.8°$ for three devices made of Ge: an homogeneous slab of the same thickness than the 9-layer photonic crystal film (approximately 8.5 μm), the 9-layer photonic crystal film, and a 9-layer photonic crystal film such that the outer layer (on the incident side) is truncated. Below $\lambda = 1.55$ μm, the emissivity of the three Ge devices is large due to the losses in the semiconductor. Over $\lambda = 1.55$ μm, the emissivity of the homogeneous slab exhibits several emission peaks, which are characteristic of a Fabry-Perot behavior. The index contrast is large between air and Ge so there are multiple reflections at the interfaces of the film. When there are constructive interferences, there is a resonance with amplified electromagnetic field inside the slab and then an emission peak. When considering the emission spectrum of the 9-layer Ge photonic crystal film (dash-dotted line), the emission peaks disappear for the wavelengths lying inside the gap as expected. The emission is then less than 0.05. We now consider the emission properties of a film of photonic crystal with a truncated outer layer of height $h_{term} = 0.1635$ μm. We can see that a sharp emission peak (equal to 0.95) appears in the gap at the wavelength $\lambda = 1.55$ μm. We will show that the enhancement of the emission is due to the resonant excitation of leaky surface waves that appear with a suitable truncation. It is clearly seen that the emission of the Ge photonic crystal can be modified and controlled by the photonic crystal structure. Indeed, the photonic crystal produces a decay of the emissivity in the desired range of wavelength. Furthermore, by using a suitable truncation of the outer layer, a peak can be produced. For both films of photonic crystal, and in the range of wavelengths over $\lambda = 1.65$ μm, we can observe several peaks of emissivity. They are due to Fabry-Perot resonances of the propagating Bloch waves inside the

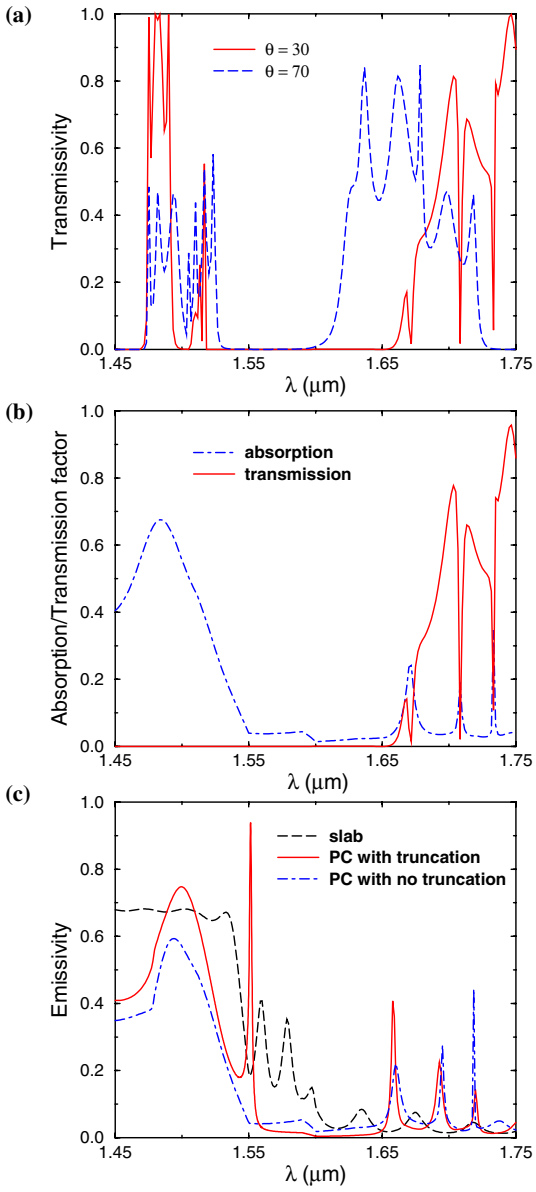

FIG. 3 (color online). Effect of the gap on the radiative properties of Ge. (a) Transmission spectrum of the photonic crystal film without losses, (b) absorption spectrum (for $\theta = 30°$) with the experimental value of the dielectric constant of the photonic crystal film (with no truncation), and (c) emission spectrum (for $\theta = 33.8°$) for three different systems: an homogeneous slab (dashed line), a photonic crystal (PC) film (dash-dotted line), and a truncated photonic crystal film (solid line).

photonic crystal film [24]. They are independent of the terminations of the film as the peaks appear at the same wavelengths for both photonic crystal films.

Figure 4 represent the emissivity of (a) a slab, (b) a 9-layer photonic crystal film without truncation, and (c) a 9-layer photonic crystal film with a truncated outer layer ($h_{term} = 0.1635$ μm) in the (ω, $k_{\|}$) plane, where ω is the frequency of the plane wave and $k_{\|}$ the wave vector component along the x direction. Dark colors correspond to a

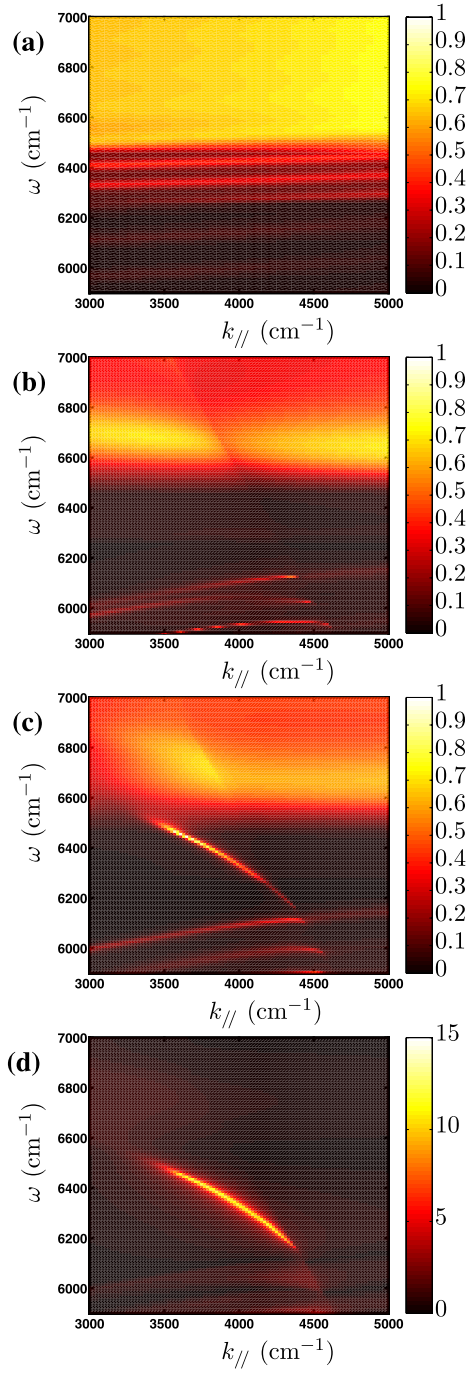

FIG. 4 (color online). Emissivity in the $(\omega, k_{\|})$ plane of (a) the slab (b) the film of 9 layers of photonic crystal without truncation, and (c) the film of 9 layers of photonic crystal with truncation. (d) represents the amplitude of the -1 order of the Rayleigh decomposition of the field at the incident side of the truncated film when illuminated by a plane wave (with amplitude equal to 1).

low emissivity, whereas bright colors correspond to a large emissivity. The upper side of the plane corresponds to frequencies larger than 6500 cm^{-1} (e.g., wavelengths lower than 1.54 μm) where the losses are large in Ge so the emission is large. In Fig. 4(a), for frequencies between 6300 cm^{-1} ($\lambda = 1.59\ \mu$m) and 6500 cm^{-1} ($\lambda = 1.54\ \mu$m), we see the emission peaks (like band stripe) due the Fabry-Perot resonance in the slab. Those peaks disappear in Fig. 4(b), because the frequencies now lie in the photonic band gap. When the film is truncated, in Fig. 4(c), an emission peak appears in the gap [the bright line between the frequencies $\omega = 6100\ \mathrm{cm}^{-1}$ (1.64 μm) and $\omega = 6452\ \mathrm{cm}^{-1}$ (1.54 μm)]. The wavelength of the emission maximum changes with $k_{\|}$, and therefore with the emission angle ($k_{\|} = \omega \sin\theta/c$). Hence, for a given wavelength, this film of photonic crystal exhibits a directional emission at an angle given by the dispersion relation.

We now discuss the origin of the emissivity peak in the gap. Owing to Kirchhoff's law, an emissivity peak coincides with an absorption peak. Thus, we analyze the structure of the field in the system when illuminated by a plane wave. The reflected field at the interface air-photonic crystal film can be written with a Rayleigh expansion (the film is periodic following the x direction):

$$E_r(x, z) = \sum_n E_n e^{i[k_{\|} + n(2\pi/a)]x} e^{i\gamma_n z}, \qquad (1)$$

where $k_{\|}$ is the incident wave vector component in the x direction and $\gamma_n^2 = \frac{\omega^2}{c^2} - (k_{\|} + n\frac{2\pi}{a})^2$ with $\mathrm{Im}(\gamma_n) > 0$ its component in the z direction. This is a Bloch wave of the form $E_r(x, z) = e^{ik_{\|}x} u_{k_{\|}}(x, z)$, where $u_{k_{\|}}(x, z) = \sum_n E_n e^{in(2\pi/a)x} e^{i\gamma_n z}$ is a periodic function of period a. Among all the orders, only the zero order is propagating in the $(\omega, k_{\|})$ domain where the emission peak of the truncated photonic crystal film exists. Figure 4(d) displays the amplitude of the -1 evanescent order in the $(\omega, k_{\|})$ plane when a plane wave is incident on the film. The amplitude of the incident wave is equal to 1. The bright colors correspond here to an amplitude larger than 10. We can observe that the maxima of the amplitude of the -1 evanescent order (larger than 10 times the amplitude of the propagating 0 order) coincide with the absorption peak. The -1 evanescent order dominates all the other orders which do not show a similar enhancement. Hence, at the resonance, the field over the photonic crystal film has a structure of a leaky surface wave with a propagating wave (the 0 order) and an amplified evanescent wave (the -1 order) to which we will refer to as surface wave. A map of the intensity of the near field over one period of the photonic crystal confirmed the structure of leaky surface wave at the absorption resonance (not shown). We observed an enhancement of the field at the interface of the photonic crystal and an exponential decay in the vacuum away from the interface. Thus, we can conclude that the absorption peak coincides with the resonant excitation of a surface wave.

In order to characterize the directivity of the thermal source, we show the angular emission spectrum at $\lambda = 1.55\ \mu$m of the three devices described previously (see

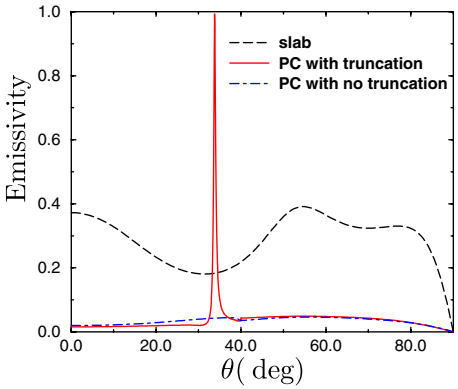

FIG. 5 (color online). Angular emissivity spectrum at $\lambda = 1.55\ \mu$m for the three systems made of Ge: the slab of thickness 8.5 μm, the photonic crystal film, and the truncated photonic crystal film.

Fig. 5). The slab exhibits a broad emission spectrum around a mean value for the emissivity of 0.3. We can also notice that the emissivity of the photonic crystal film is low for all the emission angles as the wavelength $\lambda = 1.55\ \mu$m lies in the gap. For the truncated photonic crystal film, we can observe a very narrow lobe of emission around the angle $\theta = 33.8°$, the full width at half maximum of this lobe is $\Delta\theta = 0.58°$ (10 mrad), and the emissivity is enhanced and reaches 0.95. The directivity of the source is directly linked to the spatial coherence length L_{coh} of the thermal source by $L_{\mathrm{coh}} = \lambda/(\pi\Delta\theta\cos\theta)$ [25]. The narrower the emission lobe, the more spatially coherent the thermal source. The spatial coherence is due to the presence of the surface wave which correlates the field over a distance equal to its decay length along the x direction. At a given frequency, this thermal source can thus be viewed as a thermal antenna of spatial extent equal to the propagation length of the surface wave. Here, the surface wave propagates over a distance given by $L_{\mathrm{coh}} = 38.3\lambda$ (i.e., 60 μm). These results are similar to what have been observed experimentally on a tungsten grating in the near infrared [26].

In this Letter, we have shown that a photonic crystal film can generate coherent thermal emission for a wavelength in the band gap. We have demonstrated the role of leaky surface waves on the air-photonic crystal interface in the emission process. The surface-wave dispersion relation can be engineered by varying the lattice parameters. Hence, the structure behaves as a tunable infrared antenna, emitting directional and quasimonochromatic light. Such structures are also relevant in the context of single-molecule fluorescence, in which metallic structured surfaces or nanoantennas creating local-field enhancement can be used to amplify the signal [27–29]. The advantage of the photonic crystal structure studied here is the possibility of creating frequency tunable local-field enhancement with low loss materials.

M. L. acknowledges the Délégation Générale à l'Armement for financial support. This work has been supported by the EU Integrated Project "Molecular Imaging" (EU Contract No. LSHG-CT-2003-503259).

[1] H. Sai *et al.*, J. Opt. Soc. Am. A **18**, 1471 (2001).
[2] A. Heinzel *et al.*, J. Mod. Opt. **47**, 2399 (2000).
[3] T. López-Rios *et al.*, Phys. Rev. Lett. **81**, 665 (1998); F. J. García-Vidal *et al.*, J. Lightwave Technol. **17**, 2191 (1999).
[4] R. Carminati and J.-J. Greffet, Phys. Rev. Lett. **82**, 1660 (1999).
[5] J.-J. Greffet *et al.*, Nature (London) **416**, 61 (2002).
[6] M. Kreiter *et al.*, Opt. Commun. **168**, 117 (1999).
[7] S. Y. Lin *et al.*, Phys. Rev. B **62**, R2243 (2000).
[8] S. Y. Lin, J. G. Fleming, and I. El-Kady, Appl. Phys. Lett. **83**, 593 (2003).
[9] A. Narayanaswamy and G. Chen, Phys. Rev. B **70**, 125101 (2004).
[10] S. Enoch *et al.*, Appl. Phys. Lett. **86**, 261101 (2005).
[11] O. G. Kollyukh *et al.*, Opt. Commun. **225**, 349 (2003).
[12] P. Ben-Abdallah, J. Opt. Soc. Am. A **21**, 1368 (2004).
[13] B. J. Lee, C. J. Fu, and Z. M. Zhang, Appl. Phys. Lett. **87**, 071904 (2005).
[14] R. D. Meade *et al.*, Phys. Rev. B **44**, 10 961 (1991).
[15] W. M. Robertson *et al.*, Opt. Lett. **18**, 528 (1993).
[16] F. Ramos-Mendieta and P. Halevi, Solid State Commun. **100**, 311 (1996); Phys. Rev. B **59**, 15 112 (1999).
[17] E. Moreno, F. J. García-Vidal, and L. Martin-Moreno, Phys. Rev. B **69**, 121402(R) (2004).
[18] P. Kramper *et al.*, Phys. Rev. Lett. **92**, 113903 (2004).
[19] M. Laroche, R. Carminati, and J.-J. Greffet, Phys. Rev. B **71**, 155113 (2005).
[20] E. D. Palik, *Handbook of Optical Constants of Solids* (Academic Press, San Diego, 1985).
[21] M. Plihal *et al.*, Opt. Commun. **80**, 199 (1991).
[22] N. Chateau and J.-P. Hugonin, J. Opt. Soc. Am. A **11**, 1321 (1994).
[23] J.-J. Greffet and M. Nieto-Vesperinas, J. Opt. Soc. Am. A **15**, 2735 (1998).
[24] A. Sentenac, J.-J. Greffet, and F. Pincemin, J. Opt. Soc. Am. B **14**, 339 (1997).
[25] F. Marquier *et al.*, Phys. Rev. B **69**, 155412 (2004).
[26] M. Laroche *et al.*, Opt. Lett. **30**, 2623 (2005).
[27] H. Rigneault *et al.*, Phys. Rev. Lett. **95**, 117401 (2005).
[28] J.-J. Greffet, Science **308**, 1561 (2005).
[29] P. Mühlschlegel *et al.*, Science **308**, 1607 (2005).